Electronic Supplementary Material (ESI) for Physical Chemistry Chemical Physics.

Supporting Information for

Discovery of Twin Orbital-order Phases in Ferromagnetic Semiconducting VI_3 Monolayer

Chengxi Huang[ab], Fang Wu[c], Shunli Yu*[d], Puru Jena*[a], Erjun Kan*[b]

[a] Physics Department, Virginia Commonwealth University, Richmond, VA 23284

[b] Department of Applied Physics and Institution of Energy and Microstructure, Nanjing University of Science and Technology, Nanjing, Jiangsu 210094, P. R. China

[c] College of Information Science and Technology, Nanjing Forestry University, Nanjing, Jiangsu 210037, P. R. China

[d] National Laboratory of Solid State Microstructures and School of Physics, Nanjing University, Nanjing 210093, P.R. China

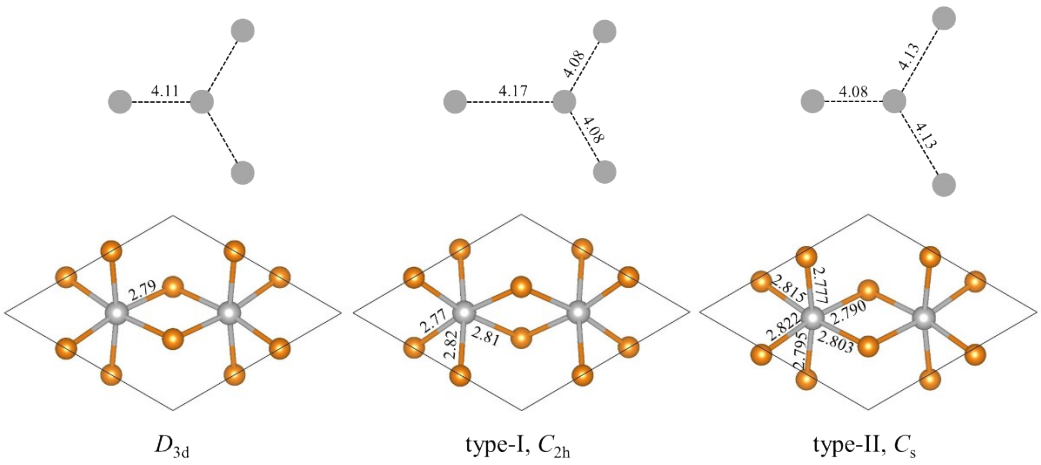

Fig. S1. The structural details for different structural phases of VI_3 monolayer. The inset labels represent the corresponding V-V and V-I bond length (in angstrom).

Following is the POSCAR files (used for VASP) for type-I and type-II phases of VI_3 monolayer.

```
Type-I
1.0
        7.1517000198          0.0000000000          0.0000000000
       -3.5418534139          6.2130578275          0.0000000000
        0.0000000000          0.0000000000         20.0000000000
   I    V
   6    2
Direct
     0.360170017           0.996910016           0.581150007
     0.003090001           0.639830000           0.418849993
     0.639829955           0.003090000           0.418849993
     0.996909944           0.360170027           0.581150007
     0.630149945           0.630149981           0.581510019
     0.369849998           0.369850008           0.418489981
     0.330649969           0.669350036           0.500000000
     0.669350028           0.330650029           0.500000000

Type-II
1.0
        7.1603999138          0.0000000000          0.0000000000
       -3.5771691193          6.2028370942          0.0000000000
        0.0000000000          0.0000000000         20.0000000000
   I    V
   6    2
Direct
     0.965569899           0.598909978           0.418389988
```

0.338979976	0.972749980	0.581749964
0.598909960	0.965569945	0.418389988
0.972749997	0.338979970	0.581749964
0.324600008	0.324599988	0.419580030
0.611570025	0.611569979	0.580519962
0.305280010	0.634729975	0.500000000
0.634729980	0.305280004	0.500000000

Table S1. Parameters derived from the maximally localized Wannier functions (MLWFs) calculated by using the wannier90 package [1]. The exchange field (U = $\varepsilon_{d\downarrow} - \varepsilon_{d\uparrow}$), crystal field ($\Delta_c = \varepsilon_{eg\uparrow} - \varepsilon_{t2g\uparrow}$), energy difference between V-*d* and I-*p* levels ($\Delta_{pd} = \varepsilon_{t2g\uparrow} - \varepsilon_{p\uparrow}$) and energy level split of t_{2g} levels [$\Delta_{t2g} = (\varepsilon_{dxy\uparrow} - \varepsilon_{dxz,yz\uparrow})/3$] for different phases of VI_3 monolayer.

	U (eV)	Δ_c (eV)	Δ_{pd} (eV)	Δ_{t2g} (eV)
D_{3d}	3.0	2.0	0.6	0
Type-I	2.8	1.6	0.5	0.47
Type-II	2.8	1.6	0.5	-0.37

Table S2. Relative energies (in eV) per unit cell for FM state of different phases of VI_3 monolayer calculated by DFT+U method (with U_{eff} = 0∼4 eV) and HSE06 functional. When U_{eff} = 0 eV, all the phases always automatically converge into D_{3d} phase. When U_{eff} = 1 eV, the C_{3i} and C_2 phase always automatically converge into type-I or type-II phases. When using HSE06 functional, the initial D_{3d} phase always automatically converge into type-I or type-II distorted phases.

Here we didn't use the energy difference between type-I and type-II phases calculated by HSE06 functional to determine the value of U_{eff}, because such energy difference is too small (≤ 0.75 meV/atom) to be reliable. Nevertheless, these results confirm the existence of twin orbital order phases of VI_3 monolayer. The reason we chose U_{eff} = 3 eV to study the properties of VI_3 monolayer is that the calculated electronic band gaps (0.86 and 0.88 eV) are very close to the experimental values (0.84∼0.9 eV).

	DFT + U_{eff} (eV)					HSE06
	0	1	2	3	4	
D_{3d}	0	0	0	0	0	---
C_{2h} (Type-I)	---	-0.063	-0.295	-0.515	-0.627	0.006
C_s (Type-II)	---	-0.068	-0.295	-0.513	-0.621	0
C_{3i}	---	---	-0.177	-0.418	-0.544	---
C_2	---	---	-0.221	-0.403	-0.524	---

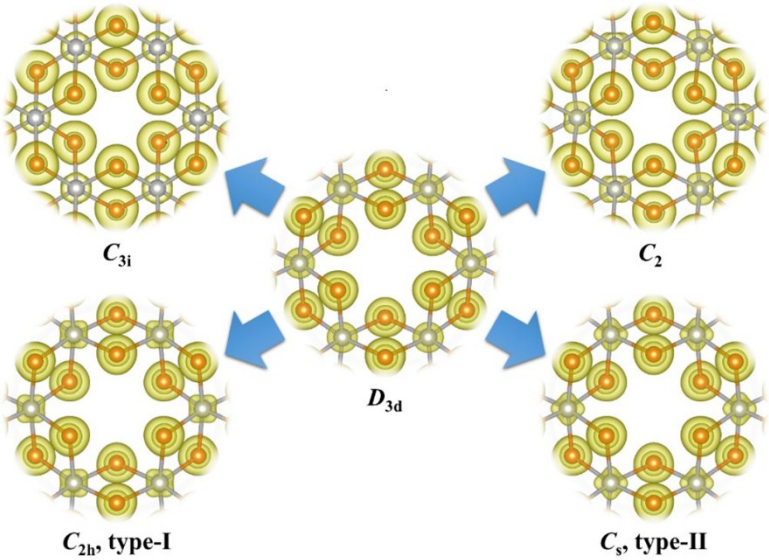

Fig. S2. Spatial charge density of VI_3 monolayer with different crystal symmetry and orbital ordering. The D_{3d} phase is studied in previous theoretical work. The C_{3i} and C_2 phases are the monolayers taken from recently experimentally observed R-3 and $C2/c$ bulk phases, respectively. The type-I and type-II phases are presented in this work.

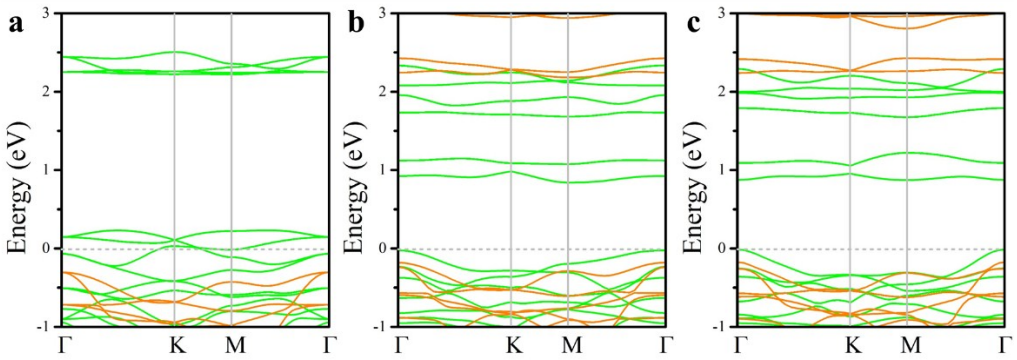

Fig. S3. Spin resolved band structures for (a) D_{3d}, (b) type-I and (c) type-II phases of VI_3 monolayer.

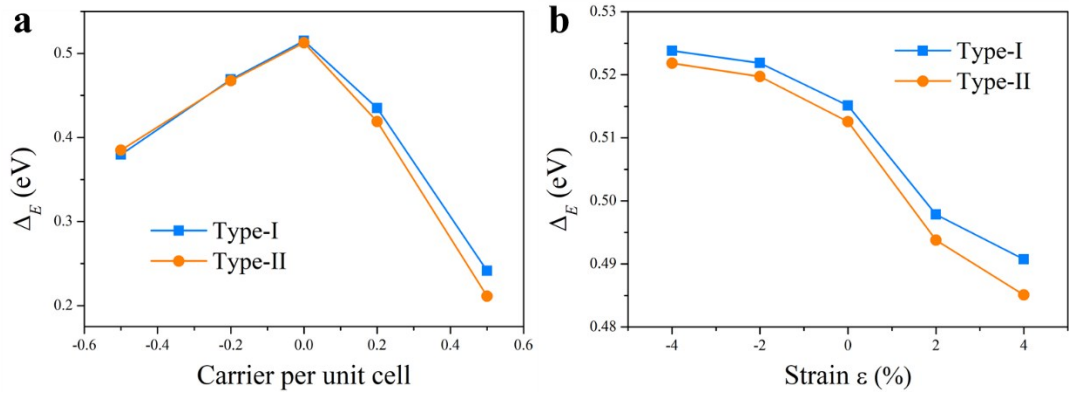

Fig. S4. Effect of (a) carrier doping and (b) in-plane external strain effect on ΔE for twin orbital-order phases of VI_3 monolayer. Negative and positive values of carrier concentration represent hole and electron doping, respectively.

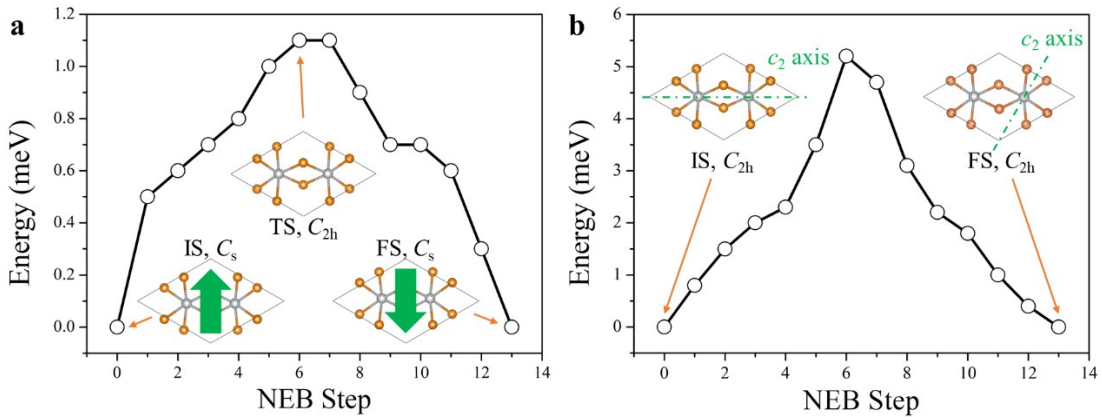

Fig. S5. (a) Ferroelectric switching along [-110] orientation for type-II VI_3 monolayer simulated by nudged-elastic-band (NEB) method. Green arrows represent the electric dipole moment. The initial state (IS) and the finial state (FS) are equivalent but have reversed ferroelectric order. The transition state (TS) has a C_{2h} structure. (b) The transition between 0° and 120° type-I phases. The IS and FS are equivalent but their in-plane c_2 axis relatively rotates by 120°.

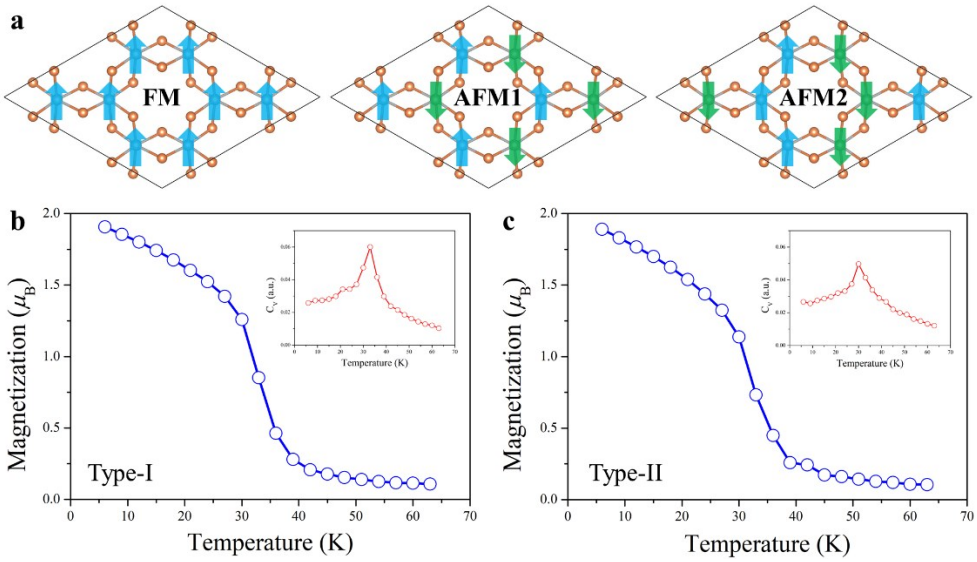

Fig. S6. (a) Considered spin configurations: The magnetizations along easy-axis direction and specific heat (Insets) as a function of temperature for (b) type-I and (b) type-II VI_3 monolayers from Monte-Carlo (MC) simulations.

According to the spin Hamiltonian

$$\hat{H} = -\frac{1}{2}\sum_i \left(J_1 \vec{S}_i \cdot \vec{S}_{i,1} + 2J_2 \vec{S}_i \cdot \vec{S}_{i,2}\right) - D\sum_i \vec{S}_{i,ez}^{\,2},$$

where the summation i runs over all the V sites, J_1 (along [110] orientation) and J_2 (along [-210] and [210] orientation) represent two different nearest-neighbor exchange parameters, D is the single-ion magnetic anisotropic parameter, $S_{i,ez}$ represents the component of S_i along the easy-axis direction and $|\boldsymbol{S}| = 1$ for the d^2 V ions. The relative energies per V for each spin configuration can be written as

$$E_{FM} = J_1 + 2J_2 + E_0$$

$$E_{AFM1} = -J_1 - 2J_2 + E_0$$

$$E_{AFM2} = -J_1 + 2J_2 + E_0$$

D can be obtained by calculating the magnetic anisotropic energy including spin-orbit coupling (SOC) effects, namely,

$$E_{FM-easy} = J_1 + 2J_2 + D + E_0$$

$$E_{FM-hard} = J_1 + 2J_2 + E_0$$

The classical Metropolis MC simulations were performed based on the above spin Hamiltonian. This method has been well examined in our previous work [2].

A 30 × 30 2D spin lattice containing 1800 spin sites with periodic boundary condition is used. During the simulation steps, each spin is rotated randomly in all directions. The average magnetization per site is taken after the system reaches equilibrium (with at least 10^5 simulation steps) state at a given temperature. The Curie temperature (T_C) is taken as the critical point of the specific heat, defined as $C_V = (\langle E^2\rangle - \langle E\rangle^2)/k_B T^2$. From Fig. S6b and c, we see that below T_C, the magnetizations are aligned along the easy-axis direction, indicating that the magnetic anisotropy is strong enough to form a long-range 2D FM order in the VI_3 monolayer.

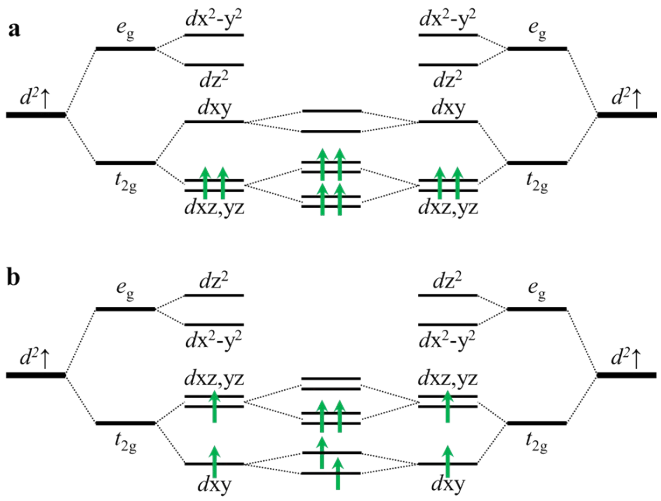

Fig. S7. Schematic diagram of orbital evolution for (a) type-I and (b) type-II phases.

Section II: The tight binding cluster model

Since structural distortions in the VI_3 monolayer are very small, and the V-I and V-V bond lengths and bond angles change only slightly. The structural distortion energy is very small (~14 meV) compared to the large stabilization energy (> 500 meV). Thus, here we omitted the structural distortions and used high-symmetric (O_h) V-I_6 octahedrons to construct the cluster model to describe the interactions between two neighboring octahedrally coordinated V ions. Based

on the mean field treatment and the linear combination of atomic orbitals method, the general Hamiltonian of the cluster is written as [4]

$$\hat{H} = \sum_{i\alpha} \epsilon_{i\alpha} \hat{d}_{i\alpha}^{\dagger} \hat{d}_{i\alpha} + \sum_{k\gamma} \epsilon_{k\gamma} \hat{p}_{k\gamma}^{\dagger} p_{k\gamma} + \sum_{i\alpha,k\gamma} \left[T_{i\alpha,k\gamma} \hat{d}_{i\alpha}^{\dagger} p_{k\gamma} + h.c. \right] + \sum_{i\alpha,j\beta} [+ \frac{U}{2} \sum_{i} \vec{e}_i \cdot \vec{S}_i$$

where α (β) represent d orbitals ($d$xy, $d$yz, $d$xz, dx^2-y^2, dz^2), γ represents p orbitals (px, py, pz), i (j) represent site index of magnetic ions, k represents site of ligand ions, respectively. The first and second terms denote the on-site energy of d and p orbitals. The third term denotes the hopping between d and p orbitals. The fourth term denotes the hopping between d orbitals. The last term is the exchange field energy of magnetic ions in an ordered ground state. Here we do not consider the spin-orbit coupling (SOC) because it barely affects the results in this system.

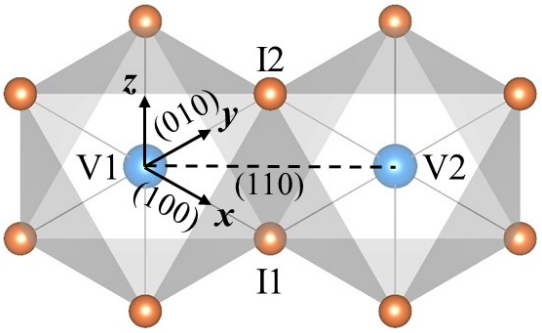

Fig. S8. The V_2I_2 cluster model.

The cluster model includes two V and two I ions, which is sufficient to describe the nearest-neighbor inter-atomic exchange interactions. Because the DFT results show that for all the systems, the FM state is the magnetic ground state. Thus, here we only considered the FM state. The Hamiltonian matrix is constructed using the atomic orbital basis {d_1x^2-y^2, d_1z^2, $d_1$xy, $d_1$yz, $d_1$xz, d_2x^2-y^2, d_2z^2, $d_2$xy, $d_2$yz, $d_2$xz, p_1x, p_1y, p_1z, p_2x, p_2y, p_2z}. In the local axis (Fig. S8), the direction cosine of the V-V bond is [l, m, n] = [$\sqrt{2}/2$, $\sqrt{2}/2$, 0], the direction cosine of four V-I bonds are [l, m,

n] = [1, 0, 0], [0, -1, 0], [0, 1, 0], [-1, 0, 0], respectively. The spin independent part of the Hamiltonian matrix can be written as

$$\hat{H}_{oct} = \begin{bmatrix} H_{M1} & T_{M1,M2} & T_{M1,L1} & T_{M1,L2} \\ T_{M2,M1} & H_{M2} & T_{M2,L1} & T_{M2,L2} \\ T_{L1,M1} & T_{L1,M2} & H_{L1} & T_{L1,L2} \\ T_{L2,M1} & T_{L2,M2} & T_{L2,L1} & H_{L2} \end{bmatrix}$$

where $H_{M1} = H_{M2} = diag\{\varepsilon_{eg}, \varepsilon_{eg}, \varepsilon_{t2g}, \varepsilon_{t2g}, \varepsilon_{t2g}\}$ are the block matrices of the intra-orbitals of the V ions. $H_{L1} = H_{L2} = diag\{\varepsilon_p, \varepsilon_p, \varepsilon_p\}$ are the block matrices of the intra-orbitals of the I ions. $T_{M1,M2}$ ($T_{M2,M1}$) is the direct exchange block matrix between V1 and V2, where the nonzero hopping integrals are given by $I_{d1x2-y2,d2x2-y2}$

$$= V_{dd\pi}, I_{d1z2,d2z2} = \frac{1}{4}(3V_{dd\delta} + V_{dd\sigma}), I_{d1xy,d2xy} = \frac{1}{4}(V_{dd\delta} + 3V_{dd\sigma}),$$

$$I_{d1xy,d2xy} = \frac{1}{4}(V_{dd\delta} + 3V_{dd\sigma}), I_{d1yz,d2yz} = I_{d1xz,d2xz} = \frac{1}{2}(V_{dd\pi} + V_{dd\delta}), I_{d1yz,d2xz} = I_{d1xz,d2yz} = \frac{1}{2}(V_{dd\pi} - V_{dd\delta}), I_{d1z2,d2xy} = I_{d1xy,d2z2} = \frac{\sqrt{3}}{4}(V_{dd\delta} - V_{dd\sigma}).$$

$T_{Mi,Li}$ (i = 1, 2) is the super-exchange block matrix between I-p orbitals and V-d orbitals. For $T_{M1,L1}$, the nonzero hopping integrals $I_{d1x2-y2,p1x} = -\frac{\sqrt{3}}{2}V_{pd\sigma}, I_{d1z2,p1x} = \frac{1}{2}V_{pd\sigma}, I_{d1xy,p1y} = I_{d1xz,p1z} = -V_{pd\pi}$. For $T_{M2,L1}$, those are $I_{d2x2-y2,p1y} = -\frac{\sqrt{3}}{2}V_{pd\sigma}, I_{d2z2,p1y} = \frac{1}{2}V_{pd\sigma}, I_{d2xy,p1x} = I_{d2yz,p1z} = -V_{pd\pi}$. According to octahedral symmetry, we have $T_{M1,L2} = -T_{M2,L1}$ and $T_{M2,L2} = -T_{M1,L1}$. The hopping among I ions hardly affects the magnetic coupling, hence we neglect $T_{L1,L2}$ ($T_{L2,L1}$). The $V_{dd\sigma}$, $V_{dd\pi}$, $V_{dd\delta}$, $V_{pd\sigma}$ and $V_{pd\pi}$ are Slater Koster hopping integrals depending on the bond length [5].

The $d$xz,yz↔e_g effective hopping integral is determined by the d-d direct-exchange and d-p-d super-exchange between $d$xz,yz and dz^2,x^2-y^2 orbitals. Because $I_{d1xz,d2z2} = I_{d1xz,d2x2-y2} = 0$, and the only nonzero d-p hopping integrals for $d$xz orbitals are $I_{d1xz,p1z}$ whereas the $I_{d2z2,p1z} = I_{d2x2-y2,p1z} = 0$; thus, the $d$xz↔e_g

effective hopping is zero, so is the effective $d$yz↔e_g hopping. For $d$xz,yz↔$d$xy exchange, $I_{d1xz,d2xy}=0$, and the $I_{d1xy,p1z}=0$, thus it is also zero. The $d$xy↔e_g effective hopping is nonzero because $I_{d1xy,d2z2}=\frac{\sqrt{3}}{4}(V_{dd\delta}-V_{dd\sigma})$ and $I_{d1xy,p1y}=-V_{pd\pi}$, $I_{d2x2-y2,p1y}=-\frac{\sqrt{3}}{2}V_{pd\sigma}$, $I_{d2z2,p1y}=\frac{1}{2}V_{pd\sigma}$. The $d$xz,yz↔$d$xz,yz effective hopping is nonzero because $I_{d1yz,d2yz}=I_{d1xz,d2xz}=\frac{1}{2}(V_{dd\pi}+V_{dd\delta}), I_{d1yz,d2xz}=I_{d1xz,d2yz}=\frac{1}{2}(V_{dd\pi}-V_{dd\delta})$ and $I_{d1xz,p1z}=I_{d2yz,p1z}=-V_{pd\pi}$. The $d$xy↔$d$xy hopping is totally from the direct hopping $I_{d1xy,d2xy}=\frac{1}{4}(V_{dd\delta}+3V_{dd\sigma})$.

Here we define the energy level difference between d and p orbitals as Δ_{pd} = $\varepsilon_{t2g}-\varepsilon_p$, the energy level split caused by octahedral crystal field as $\Delta_c=\varepsilon_{eg}-\varepsilon_{t2g}$, the energy level split of t_{2g} levels as $\Delta_{t2g}=|\varepsilon_{dxy}-\varepsilon_{dxz,yz}|/3$. Using a coefficient t_0 evaluate the strength of the super-exchange and direct-exchange interactions, we set $V_{dd\sigma}=-t_0$, $V_{dd\pi}=0.25t_0$, $V_{dd\delta}=0.125t_0$, $V_{pd\sigma}=-4t_0$ and $V_{pd\pi}=1.6t_0$. The electron configuration for the V_2I_2 cluster is $p^{12}d^4$ (4 spin up d, 6 spin up p and 6 spin down p electrons). Thus, the energy of FM state can be obtained by summarizing the 16 lowest eigenvalues from the numerically diagonalized corresponding Hamiltonian matrix. For the high-symmetric case, Δ_{t2g} =0; for the type-I case, $\varepsilon_{dxy}=\varepsilon_{t2g}+2\Delta_{t2g}$, and $\varepsilon_{dxz,yz}=\varepsilon_{t2g}-\Delta_{t2g}$; for the type-II case, $\varepsilon_{dxy}=\varepsilon_{t2g}-2\Delta_{t2g}$, and $\varepsilon_{dxz,yz}=\varepsilon_{t2g}+\Delta_{t2g}$. For Fig. 1b presented in the main text, the default values for U, Δ_c, Δ_{pd} and Δ_{t2g} and t_0 are taken as 3, 1.8, 0.5 and 0.5 eV, respectively. These values are comparable to those derived from the MLWFs results (see table S1).

When the Δ_{t2g} increases from 0.5 to 1.5 eV or $V_{pd\sigma}$ and $V_{pd\pi}$ are reduced by 50%, the crossing between the type-I and type-II profiles disappears and the type-I phase becomes always more preferred than the type-II phase. These indicate that, in a VI_3-like system, when the on-site splitting is stronger and/or the super-

exchange is weaker (compared with the direct-exchange), the type-I phase will be more preferred than the type-II phase. That is to say, only when the JT effect is rather weak and the super-exchange interaction is relatively strong, the twin orbital-order effect may occur in a VI_3-like system.

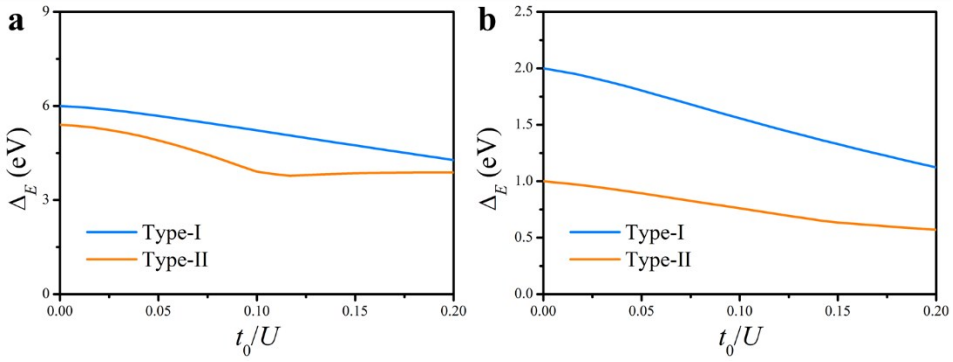

Fig. S9. Stabilization energy ($\Delta E = E_{D3d} - E_{\text{type-I or type-II}}$) as a function of t_0/U. For (a), Δ_{t2g} is set to 1.5 eV. For (b), $V_{pd\sigma} = -2t_0$ and $V_{pd\pi} = 0.8t_0$.

Section III: Other VI_3-like systems

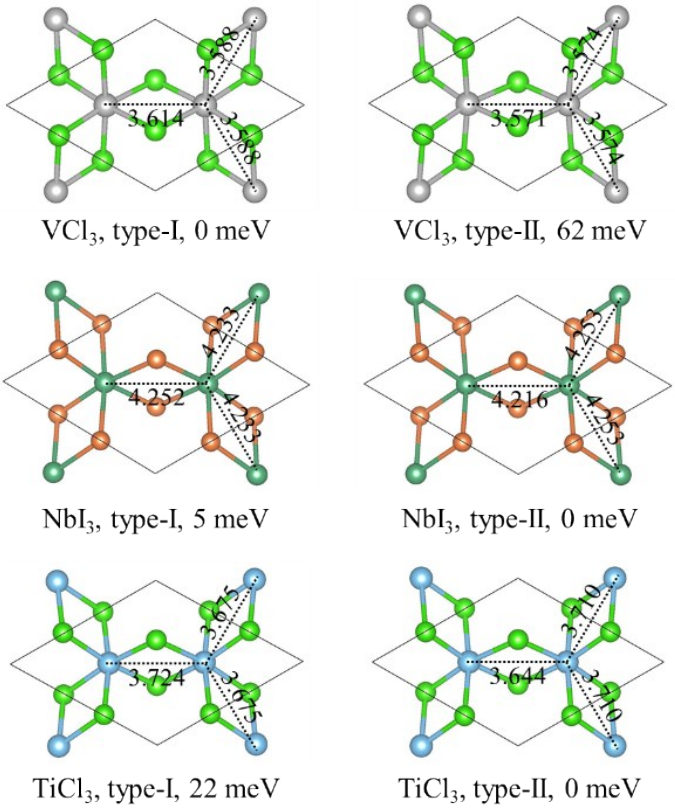

VCl_3, type-I, 0 meV

VCl_3, type-II, 62 meV

NbI_3, type-I, 5 meV

NbI_3, type-II, 0 meV

$TiCl_3$, type-I, 22 meV

$TiCl_3$, type-II, 0 meV

Fig. S10. The structural details and relative energies of different structural phases of VCl_3, NbI_3 and $TiCl_3$ monolayers. The inset labels represent the corresponding metal-metal bond length (in angstrom).

DFT+*U* method was used in the calculations for these systems. U_{eff} = 3 eV was adopted for V-*d* and Ti-*d* orbitals, and U_{eff} = 2 eV was adopted for Nb-*d* orbitals.

References:

[1] A. A. Motofi, J. R. Yates, G. Pizzi, Y. S. Lee, I. Souza, D. Vanderbilt, N. Marzari, An updated version of Wannier90: A Tool for Obtaining Maximally Localised Wannier Functions. *Comput. Phys. Commun*. **185**, 2309 (2014).

[2] C. Huang, Y. Du, H. Wu, H. Xiang, K. Deng, and E. Kan, Prediction of Intrinsic Ferromagnetic Ferroelectricity in a Transition-Metal Halide Monolayer. *Phys. Rev. Lett.* 120, 147601 (2018).

[3] C. Huang, J. Feng, F. Wu, D. Ahmed, B. Huang, H. Xiang, K. Deng, and E. Kan, Toward Intrinsic Room-Temperature Ferromagnetism in Two-Dimensional Semiconductors. *J. Am. Chem. Soc.*, 140, 11519–11525 (2018).

[4] H. Katsura, N. Nagaosa, A. V. Balatsky, Spin Current and Magnetoelectric Effect in Noncollinear Magnets. *Phys. Rev. Lett.* **95**, 057205 (2005).

[5] J. C. Slater, G. F. Koster, Simplified LCAO Method for the Periodic Potential Problem. Phys. Rev. **94**, 1498 (1954).